

Full length article

## New insights on a sign-switching $\Lambda$

Jorge F. Soriano<sup>a</sup>, Shimon Wohlberg<sup>a,b</sup>, Luis A. Anchordoqui<sup>a,b,c,\*</sup>

<sup>a</sup> Department of Physics, Lehman College, City University of New York, NY 10468, USA

<sup>b</sup> Department of Astrophysics, American Museum of Natural History, NY 10024, USA

<sup>c</sup> Department of Physics, Graduate Center, City University of New York, NY 10016, USA

### ARTICLE INFO

#### Keywords:

$H_0$  and  $S_8$  tensions

### ABSTRACT

The proposal for a sudden sign-switching cosmological constant  $\Lambda$  in the local universe, emulating a phase transition from anti-de Sitter (AdS) to de Sitter (dS) space, has markedly revamped the fit to observational data and lays out a propitious framework for ameliorating major cosmological tensions, such as the  $H_0$  and  $S_8$  tensions. This proposal is widely known as  $\Lambda_s$ CDM. We investigate the possibility that  $\Lambda$  does not only flip sign at the transition but has also different curvature radii in the AdS and dS phases. We show that the critical redshift of the transition  $z_c$  is strongly correlated with the vacuum energy in the AdS phase  $\Omega_{\Lambda_s}$ , and that these two variables do not correlate strongly with the other cosmological parameters. We also show that the cost of adding an additional parameter to the  $\Lambda_s$ CDM cosmological model does not improve the goodness of fit. Armed with our findings, we demonstrate that for a proper choice of  $z_c$ , the vacuum energy in the dS phase may not necessarily be  $-\Omega_{\Lambda_s}$ , for comparable degree of conformity between the model prediction and experimental data.

### 1. Introduction

A cold dark matter ( $\Lambda$ CDM) has proven incredibly successful at describing many features of cosmology that we observe in our experiments [7]. The most famous example, arguably, is the agreement with data from the cosmic microwave background (CMB) [8]. Yet, with the increase in precision of cosmological observations over the past decade, this success has been challenged. Two of the most compelling shortcomings of  $\Lambda$ CDM are its predictions of the present-day expansion rate  $H_0$  and the amplitude of the matter clustering in the late Universe (parameterized by  $S_8$ ) [9]. Strictly speaking, the values  $H_0 = 67.4 \pm 0.5$  km/s/Mpc and  $S_8 = 0.834 \pm 0.016$  inferred from *Planck*'s CMB data assuming  $\Lambda$ CDM [8] are in  $\sim 5\sigma$  tension with  $H_0 = 73.04 \pm 1.04$  km/s/Mpc from the SH0ES distance ladder measurement (using Cepheid-calibrated type-Ia supernovae) [10,11] and in  $\sim 3\sigma$  tension with  $S_8 = 0.766^{+0.020}_{-0.014}$  from the cosmic shear data of the Kilo-Degree Survey (KiDS-1000) [12], respectively. Systematic effects do not seem to be responsible for these discrepancies (see e.g. [13]), which have become a new cornerstone of theoretical physics. Naturally, many new physics setups are rising to the challenge [14–17].

$\Lambda_s$ CDM [18–21] is one of the many new physics setups that have been proposed to simultaneously accommodate the  $H_0$  and  $S_8$  tensions.<sup>1</sup> The setup relies on an empirical conjecture which postulates

that  $\Lambda$  may have switched sign (from negative to positive) at critical redshift  $z_c \sim 2$ ;

$$\Lambda \rightarrow \Lambda_s \equiv \Lambda_0 \operatorname{sgn}(z_c - z), \quad (1.1)$$

with  $\Lambda_0 > 0$ , and where  $\operatorname{sgn}(x) = -1, 0, 1$  for  $x < 0$ ,  $x = 0$  and  $x > 0$ , respectively. Apart from resolving the three major cosmological tensions,  $\Lambda_s$ CDM achieves quite a good fit to Lyman- $\alpha$  data provided  $z_c \lesssim 2.3$  [18], and it is in agreement with the otherwise puzzling JWST observations [22,23].

The colossal success of  $\Lambda_s$ CDM in accommodating observations of baryon acoustic oscillations (BAO) is in effect contingent on the (angular) transversal two dimensional (2D) BAO data on the shell, which are less model dependent than the 3D BAO data. This is because the 3D BAO data sample relies on  $\Lambda$ CDM to determine the distance to the spherical shell, and hence could potentially introduce a bias when analyzing cosmological scenarios beyond  $\Lambda$ CDM [24,25]. Indeed, by using 2D BAO data the actual SH0ES  $H_0$  measurement and the angular diameter distance to the last scattering surface can be simultaneously accommodated, but at the expense of having an effective negative energy density for  $z \gtrsim 2$ .

Another caveat associated to  $\Lambda_s$ CDM is that the instantaneous transition of the vacuum energy density, which is governed by the signum

\* Corresponding author at: Department of Physics, Lehman College, City University of New York, NY 10468, USA.

E-mail addresses: [jorge.soriano@lehman.cuny.edu](mailto:jorge.soriano@lehman.cuny.edu) (J.F. Soriano), [shimon.wohlberg@lc.cuny.edu](mailto:shimon.wohlberg@lc.cuny.edu) (S. Wohlberg), [luis.anchordoqui@gmail.com](mailto:luis.anchordoqui@gmail.com)

(L.A. Anchordoqui).

<sup>1</sup> For related works, see [1–4]. An alternative model that simultaneously addresses  $H_0$  and  $S_8$  is discussed in [5,6].

function, gives rise to a hidden sudden singularity at  $z_c$  [26]. Note that the scale factor  $a$  of  $\Lambda_s$ CDM is continuous and non-zero at the critical time  $t = t_c$ , but its first derivative  $\dot{a}$  is discontinuous, and its second derivative  $\ddot{a}$  diverges. However, the sudden singularity yields a minimal impact on the formation and evolution of cosmic bound structures, thereby preserving the viability of  $\Lambda_s$ CDM [27].

The changeover of  $\Lambda$  at  $z_c$  can be interpreted as a phase transition between anti-de Sitter (AdS) and (dS) spaces, because  $n$ -dimensional dS and AdS spaces can be regarded as solutions of Einstein's field equations of empty spaces with cosmological constant

$$\Lambda = (n-2)R_i/(2n), \quad (1.2)$$

where  $i = \{dS_n, AdS_n\}$ ,  $R_{dS_n} = n(n-1)/\ell_{dS_n}^2$  and  $R_{AdS_n} = -n(n-1)/\ell_{AdS_n}^2$  are respectively the dS and AdS Ricci scalars, and  $\ell_i$  is the radius of curvature [28].

The essence of the instantaneous sign-switching cosmological constant posits a challenging puzzle in identifying a concrete theoretical model able to accommodate the AdS  $\rightarrow$  dS transition. The puzzle is actually exacerbated by the AdS distance conjecture, which states that there is an arbitrarily large distance between AdS and dS vacua in metric space [29]. Having said that, the phenomenological success of  $\Lambda_s$ CDM, despite its simplistic structure, provides robust motivation to search for possible underlying physical mechanisms to describe the conjectured AdS  $\rightarrow$  dS transition. Many theoretical realizations have been proposed [30–39]. Motivated by the phenomenological success of  $\Lambda_s$ CDM, in this paper we investigate the possibility that  $\Lambda$  does not only flip sign at the transition but has also different curvature radii in the AdS and dS phases. In plain English, the AdS radius  $\ell_{AdS_d}$  characterized by  $\Lambda_-$  and the dS radius  $\ell_{dS_d}$  characterized by  $\Lambda_+$  satisfy  $|\Lambda_-| \neq |\Lambda_+|$ .

The layout of the paper is as follows. In Section 2 we introduce the cosmological parameters explored in this work. In Section 3 we describe the analysis method and the observational datasets/likelihoods used to constrain the cosmological parameters. After that we implement the numerical computations, present our results, and discuss their implications. The paper wraps up in Section 4 with some conclusions.

## 2. Cosmological parameters

There are two basic hypotheses in modern cosmology: (i) the assumption of the validity of General Relativity and (ii) the cosmological principle, which is the assumption that the universe on cosmological scales is homogeneous and isotropic. Together, these two hypotheses set constraints on the four-dimensional spacetime metric, which reduces to the maximally-symmetric Friedmann–Lemaître–Robertson–Walker line element

$$ds^2 = -dt^2 + a^2(t) \left[ \frac{dr^2}{1-kr^2} + r^2(d\theta^2 + \sin^2\theta d\phi^2) \right], \quad (2.1)$$

where  $(t, r, \theta, \phi)$  are co-moving coordinates,  $k (= -1, 0, 1)$  parametrizes the curvature of the homogeneous and isotropic spatial sections, and  $a(t)$  is the cosmic scale factor, which is related to the redshift  $z$  by  $a = 1/(1+z)$  [40]. Observations favor a spatially flat ( $k = 0$ ) universe [7]. The expansion rate of the Universe is measured by the Hubble parameter,

$$H = \frac{\dot{a}}{a}, \quad (2.2)$$

and its present-day value is known as the Hubble constant  $H_0 = 100 h$  km/Mpc/s, with  $0 < h < 1$  [41].

The widely accepted spatially-flat  $\Lambda$ CDM model requires only 6 independent parameters

$$\mathcal{P}_{\Lambda\text{CDM}} = \{\omega_b, \omega_{cdm}, \theta_s, \tau_{\text{reio}}, n_s, A_s\}, \quad (2.3)$$

to completely specify the cosmological evolution, where  $\omega_b \equiv \Omega_b h^2$  is the baryon density,  $\omega_{cdm} \equiv \Omega_c h^2$  is the CDM density,  $\theta_s$  is the angular size of the sound horizon at recombination,  $\tau_{\text{reio}}$  is the Thomson

scattering optical depth due to reionization,  $n_s$  is the scalar spectral index, and  $A_s$  is the power spectrum amplitude of adiabatic scalar perturbations. The  $\Omega_i$  parameters are defined as the ratio of the present day mean density of each component  $i$  to the critical density; by definition  $\sum_i \Omega_i = 1$ . Neglecting smaller order terms,  $\Omega_c + \Omega_b + \Omega_\Lambda \sim 1$ .

The specific set of six parameters used to define the cosmological model is somewhat open to choice. Within the context of fitting a  $\Lambda$ CDM model to a CMB power spectrum, the six selected key parameters are primarily chosen to avoid degeneracies and thus speed convergence of the model fit to the data [42–44]. Other interesting parameters providing additional physical insight may be derived from the model once the defining six parameters have been set. These include:

- The present-day expansion rate  $H_0$ .
- The amplitude of the matter clustering in the late universe, parameterized by

$$S_8 \equiv \sigma_8 \left( \frac{\Omega_m}{0.3} \right)^{0.5}, \quad (2.4)$$

where  $\sigma_8$  is the root mean square of the amplitude of matter perturbations smoothed over  $8 h^{-1}$ Mpc and  $\Omega_m = \Omega_c + \Omega_b$  is the non-relativistic matter density.

- The effective number of relativistic neutrino-like species  $N_{\text{eff}}$  is a convenient parametrization of the relativistic energy density of the universe beyond that of photons, in units of the density of a single Weyl neutrino species [45]. Using conservation of entropy, fully thermalized relics with  $g_*$  degrees of freedom contribute

$$N_{\text{eff}} = 3.043 + g_* \left( \frac{43}{4g_*} \right)^{4/3} \begin{cases} 4/7 & \text{for bosons} \\ 1/2 & \text{for fermions} \end{cases}, \quad (2.5)$$

where 3.043 is the standard-model benchmark [46] and  $g_*$  denotes the effective degrees of freedom for the entropy of the other thermalized relativistic species that are present when they decouple [47].<sup>2</sup>

Herein, we aim to explore possible deviations from  $\Lambda$ CDM. To quantitatively assess these deviations we study the  $\Lambda_s$ CDM 7-parameter model,

$$\mathcal{P}_{\Lambda_s\text{CDM}} = \{\omega_b, \omega_{cdm}, \theta_s, \tau_{\text{reio}}, n_s, A_s, z_c\}, \quad (2.6)$$

and the  $\Lambda_{\mp}$ CDM 8-parameter model

$$\mathcal{P}_{\Lambda_{\mp}\text{CDM}} = \{\omega_b, \omega_{cdm}, \theta_s, \tau_{\text{reio}}, n_s, A_s, z_c, \Omega_{\Lambda_{\mp}}\}. \quad (2.7)$$

As might be expected, for both these models the first six parameters are common ones with  $\Lambda$ CDM.

Before proceeding, we pause to mention additional, non-cosmological parameters that are included in the model. First, there are 53 nuisance parameters needed to characterize the Planck and KiDS-1000 likelihoods, described in the next section. More importantly, the absolute magnitude of type Ia supernovae  $M_B$  (needed for the Pantheon+ likelihood; see next section), must be considered too. It has been suggested that the  $H_0$  tension is actually a tension on  $M_B$  [54,55], because the base  $\Lambda$ CDM cosmology inferred from *Planck* leads to  $M_B = -19.401 \pm 0.027$  mag [56], whereas the SH0ES Cepheid photometry and Pantheon supernova peak magnitudes yield  $M_B = -19.244 \pm 0.037$  mag [55]. It has been shown that  $\Lambda_s$ CDM cosmology provides a robust solution to the  $M_B$  tension [21].

We consider two scenarios with  $N_{\text{eff}} = 3.043$  and  $N_{\text{eff}} = 3.294$ . The latter characterizes a model that explains the AdS  $\rightarrow$  dS transition using the contribution to the Casimir energy of fields (the graviton, a real scalar, and three right-handed neutrinos) propagating in the bulk of a five-dimensional spacetime [30]. The scalar field has a potential holding two local minima with very small difference in vacuum energy and bigger curvature (mass) of the lower one, and thus when the false

<sup>2</sup> We adopt the most recent NLO calculation of  $N_{\text{eff}}$  in the standard model [46], which yields a reduction from previous estimates [48–53].

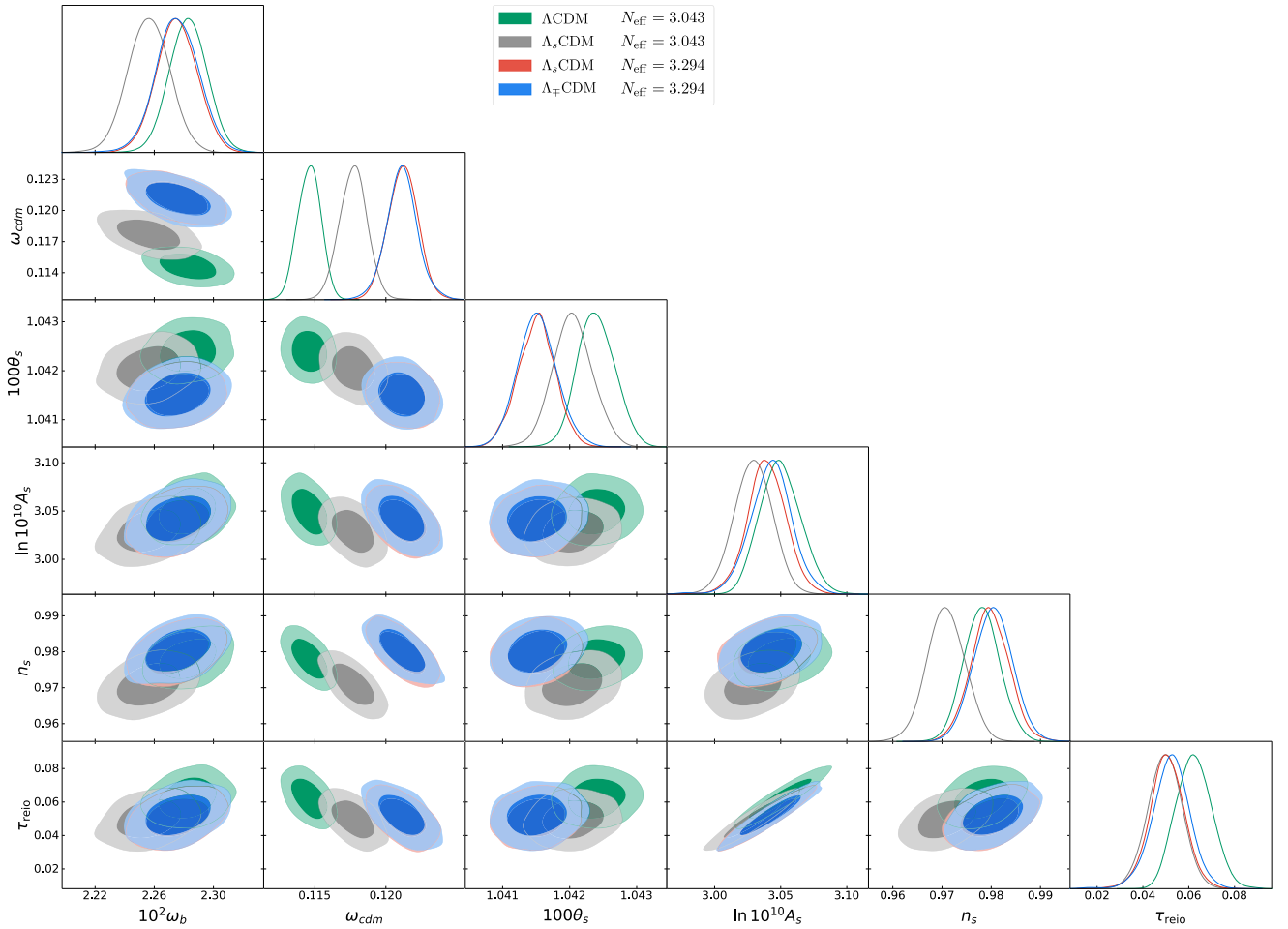


Fig. 1. Triangle plot showing two-dimensional contours at 68% and 95% CL and one-dimensional posterior probability distribution functions of the six parameters which are common to  $\Lambda$ CDM,  $\Lambda_s$ CDM, and  $\Lambda_{\pm}$ CDM.

vacuum tunnels to its true vacuum state, the field becomes more massive and its contribution to the Casimir energy becomes exponentially suppressed [37]. The tunneling process then changes the difference between the total number of fermionic and bosonic degrees of freedom contributing to the quantum corrections of the vacuum energy in a way that leads to a sign-switching cosmological constant at  $z_c \sim 2$ .

### 3. Statistical methodology, observational data, and numerical analysis

We adopt the Markov Chain Monte Carlo (MCMC) technique. A (discrete-time) Markov chain with (finite or countable) state space  $\mathcal{X}$  consists of a sequence  $X_0, X_1, \dots$  of  $\mathcal{X}$ -valued random variables such that for all states  $i, j, k_0, k_1 \dots$  and all times  $n = 0, 1, 2, \dots$ ,

$$P(X_{n+1} = j \parallel X_n = i, X_{n-1} = k_{n-1}, \dots) = p(i, j) \quad (3.1)$$

where  $p(i, j)$  depends only on the states  $i, j$ , and not on the time  $n$  or the previous states  $k_{n-1}, k_{n-2}, \dots$ . The numbers  $p(i, j)$  are called the transition probabilities of the chain. Note that each number is stochastically obtained from the previous number without explicitly being dependent on it. In our analysis the states of a chain consist on specific values of the free parameters in a given cosmological model.

To run the MCMC we adopt the MontePython code, which interfaces with the Cosmic Linear Anisotropy Solving System CLASS [57–59]. To explore the full parameter space of the models characterized by (2.6) and (2.7) we have modified CLASS to introduce the possibility of an AdS  $\rightarrow$  dS transition. We derive constraints on the cosmological parameters of these two models and  $\Lambda$ CDM from data-sets and

likelihoods given below using the Metropolis–Hastings algorithm [60], while enforcing the so-called Gelman–Rubin convergence criterion of  $R-1 < 10^{-2}$  in all the runs [61]. We make use of a series of astrophysical and cosmological probes to construct our reference dataset:

- **2018 Planck CMB data:** The CMB temperature, polarization, and lensing angular power spectra from the *Planck* 2018 legacy release [8,62].
- **Transversal BAO:** Measurements of 2D baryon acoustic oscillations (BAO),  $\theta_{\text{BAO}}(z)$ , obtained in a weakly model-dependent approach, and compiled in Table I of [63].
- **Pantheon+:** The 1701 light curves of 1550 distinct supernovae type Ia, which are distributed in the redshift interval  $0.001 \leq z \leq 2.26$  [64]. We incorporate the most recent SHOES Cepheid host distance anchors [10] into the likelihood function by integrating distance modulus measurements of the Pantheon+ supernovae.
- **Cosmic Shear:** KiDS-1000 data [65,66], including the weak lensing two-point statistics data for both the auto and cross-correlations across five tomographic redshift bins [67]. We follow the KiDS team analysis and adopt the COSEBIs (Complete Orthogonal Sets of E/B-Integrals) likelihood [68]. Non-linearities are implemented into the analysis using HALOFIT [69,70].<sup>3</sup>

<sup>3</sup> This implementation comes up with a difference to the data analysis carried out in [21] (which was executed using the HMcode [71]), but such a difference leads to (almost) negligible effects in the results.

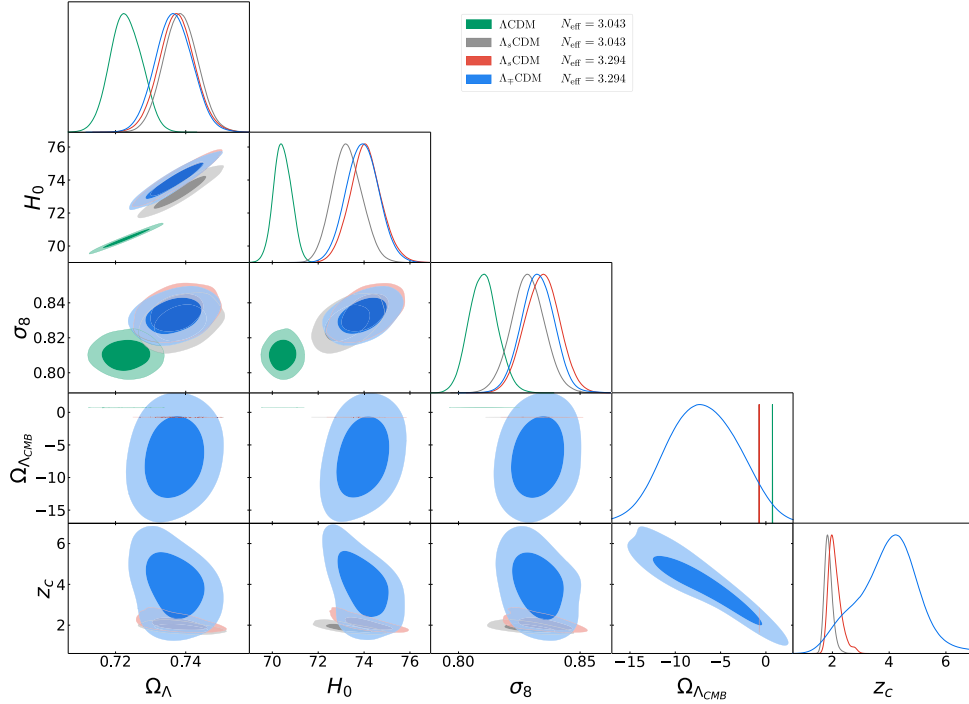


**Fig. 2.** Triangle plot showing two-dimensional contours at 68% and 95% CL and one-dimensional posterior probability distribution functions of  $H_0$ ,  $\sigma_8$ ,  $\Omega_\Lambda$ , and  $\Omega_{\Lambda_{\text{CMB}}}$  for  $\Lambda\text{CDM}$ ,  $\Lambda_s\text{CDM}$ , and  $\Lambda_\mp\text{CDM}$ . (For interpretation of the references to colour in this figure legend, the reader is referred to the web version of this article.)

**Table 1**

Marginalized constraints, mean values with 68% CL (95% CL), on the free and some derived parameters of the  $\Lambda\text{CDM}$ ,  $\Lambda_s\text{CDM}$  and  $\Lambda_\mp\text{CDM}$  models for different values of ( $N_{\text{eff}}$ ).

Model	$\Lambda\text{CDM}(3.043)$	$\Lambda_s\text{CDM}(3.043)$	$\Lambda_s\text{CDM}(3.294)$	$\Lambda_\mp\text{CDM}(3.294)$
$10^2\omega_b$	$2.283^{+0.013}_{-0.013} ({}^{+0.024}_{-0.025})$	$2.256^{+0.014}_{-0.014} ({}^{+0.028}_{-0.028})$	$2.275^{+0.014}_{-0.014} ({}^{+0.027}_{-0.027})$	$2.276^{+0.014}_{-0.014} ({}^{+0.028}_{-0.029})$
$\omega_{\text{cdm}}$	$0.1146^{+0.0008}_{-0.00083} ({}^{+0.00151}_{-0.00154})$	$0.11771^{+0.00093}_{-0.00099} ({}^{+0.0019}_{-0.00197})$	$0.1212^{+0.001}_{-0.0011} ({}^{+0.002}_{-0.002})$	$0.1211^{+0.001}_{-0.0011} ({}^{+0.0023}_{-0.0022})$
$100\theta_s$	$1.0424^{+0.00026}_{-0.0003} ({}^{+0.00055}_{-0.00052})$	$1.04204^{+0.0003}_{-0.00029} ({}^{+0.0006}_{-0.00056})$	$1.04151^{+0.00027}_{-0.00029} ({}^{+0.00054}_{-0.00056})$	$1.04152^{+0.00029}_{-0.00029} ({}^{+0.0006}_{-0.00056})$
$\ln 10^{10} A_s$	$3.05^{+0.015}_{-0.016} ({}^{+0.03}_{-0.029})$	$3.029^{+0.015}_{-0.014} ({}^{+0.028}_{-0.03})$	$3.039^{+0.015}_{-0.014} ({}^{+0.029}_{-0.03})$	$3.042^{+0.016}_{-0.015} ({}^{+0.033}_{-0.033})$
$n_s$	$0.9781^{+0.0035}_{-0.0037} ({}^{+0.0074}_{-0.007})$	$0.9708^{+0.0039}_{-0.0039} ({}^{+0.0076}_{-0.0076})$	$0.9798^{+0.004}_{-0.0037} ({}^{+0.0078}_{-0.0076})$	$0.9804^{+0.0039}_{-0.004} ({}^{+0.0077}_{-0.0077})$
$\tau_{\text{reio}}$	$0.0624^{+0.0077}_{-0.0082} ({}^{+0.0151}_{-0.0149})$	$0.0496^{+0.0074}_{-0.0073} ({}^{+0.0144}_{-0.0155})$	$0.0505^{+0.0075}_{-0.007} ({}^{+0.0152}_{-0.0158})$	$0.0521^{+0.0083}_{-0.0075} ({}^{+0.0159}_{-0.0177})$
$\Omega_\Lambda$	$0.723^{+0.0047}_{-0.0045} ({}^{+0.0085}_{-0.0085})$	$0.7386^{+0.0049}_{-0.0048} ({}^{+0.0096}_{-0.0095})$	$0.7375^{+0.0051}_{-0.0049} ({}^{+0.0103}_{-0.01})$	$0.7367^{+0.0053}_{-0.0051} ({}^{+0.0102}_{-0.0101})$
$\Omega_{\Lambda_{\text{CMB}}}$	$0.723^{+0.0047}_{-0.0045} ({}^{+0.0085}_{-0.0085})$	$-0.7386^{+0.0048}_{-0.0049} ({}^{+0.0095}_{-0.0096})$	$-0.7375^{+0.0049}_{-0.0051} ({}^{+0.01}_{-0.0103})$	$-6.9^{+3.9}_{-4.} ({}^{+6.5}_{-6.3})$
$z_c$	–	$1.86^{+0.11}_{-0.16} ({}^{+0.3}_{-0.27})$	$2.09^{+0.14}_{-0.26} ({}^{+0.49}_{-0.39})$	$4.^{+1.12}_{-0.96} ({}^{+1.97}_{-2.35})$
$M_B$ [mag]	$-19.356^{+0.01}_{-0.011} ({}^{+0.021}_{-0.021})$	$-19.279^{+0.017}_{-0.018} ({}^{+0.034}_{-0.033})$	$-19.256^{+0.018}_{-0.018} ({}^{+0.037}_{-0.035})$	$-19.26^{+0.018}_{-0.019} ({}^{+0.037}_{-0.037})$
$H_0$ [km/s/Mpc]	$70.45^{+0.38}_{-0.4} ({}^{+0.77}_{-0.76})$	$73.26^{+0.62}_{-0.68} ({}^{+1.31}_{-1.24})$	$74.07^{+0.68}_{-0.68} ({}^{+1.43}_{-1.31})$	$73.93^{+0.69}_{-0.69} ({}^{+1.42}_{-1.39})$
$\sigma_8$	$0.8102^{+0.0055}_{-0.0062} ({}^{+0.0119}_{-0.0111})$	$0.8286^{+0.0069}_{-0.0068} ({}^{+0.0139}_{-0.0138})$	$0.8344^{+0.0069}_{-0.0072} ({}^{+0.0137}_{-0.014})$	$0.8326^{+0.0066}_{-0.0065} ({}^{+0.0131}_{-0.0133})$

Our results are encapsulated in Figs. 1 and 2, and Table 1. There, for the sake of compactness,  $\Omega_\Lambda$  has its standard meaning for  $\Lambda\text{CDM}$  and  $\Lambda_s\text{CDM}$ , and it is  $\Omega_{\Lambda_+}$  for  $\Lambda_\mp\text{CDM}$ . Similarly,  $\Omega_{\Lambda_{\text{CMB}}}$  stands for  $\Omega_\Lambda$  in  $\Lambda\text{CDM}$ , for  $-\Omega_\Lambda$  in  $\Lambda_s\text{CDM}$ , and for  $\Omega_{\Lambda_-}$  in  $\Lambda_\mp\text{CDM}$ . For this reason, some of these parameters are not independent from each other (that is, they are 100% correlated), making some of the numbers in Table 1 redundant.

It is straightforward to see that the fitted parameters of  $\Lambda_s\text{CDM}$  and  $\Lambda_\mp\text{CDM}$  are all consistent with each other at 95%CL, independent of the value of  $N_{\text{eff}}$ . Moreover, for  $N_{\text{eff}} = 3.294$ , they are effectively indistinguishable in regards to the six base parameters, as well as the derived  $H_0$  and  $\sigma_8$ . This implies that scenarios with  $N_{\text{eff}} = 3.294$  can simultaneously resolve the  $H_0$  and  $S_8$  tensions. For  $\Lambda\text{CDM}$ , we find  $\chi^2_{\text{min}} = 4224.7$ . For  $\Lambda_s\text{CDM}$ , the goodness of fit always improves with respect to  $\Lambda\text{CDM}$ ; namely, if  $N_{\text{eff}} = 3.043$  we find  $\chi^2_{\text{min}} = 4192.08$ ,

whereas if  $N_{\text{eff}} = 3.294$  we find  $\chi^2_{\text{min}} = 4195.94$ .<sup>4</sup> On the other hand, while there is an improvement in the chi-squared fit of  $\Lambda_\mp\text{CDM}$  when compared to  $\Lambda\text{CDM}$ , there is no improvement in the  $\chi^2_{\text{min}}$  when  $\Lambda_\mp\text{CDM}$  with  $N_{\text{eff}} = 3.294$  is compared to  $\Lambda_s\text{CDM}$ .<sup>5</sup> We conclude that by adding the curvature radius in the AdS phase as a free model parameter we do not make better the fit to the data.

In Fig. 2, due to the large plot range needed to show the  $\Omega_{\Lambda_{\text{CMB}}}$  distribution for  $\Lambda_\mp\text{CDM}$ , the corresponding distributions for  $\Lambda\text{CDM}$  and  $\Lambda_s\text{CDM}$  apparently collapse into a line. Specifically, the  $\Lambda\text{CDM}$  (green) and  $\Lambda_s\text{CDM}$  (overlapping red and gray, not always distinguishable) lines

<sup>4</sup> There is a difference of decimal digits with respect to the  $\chi_{\text{min}}$  reported in [32], where a LO  $N_{\text{eff}} = 3.044$  was used.

<sup>5</sup> We note in passing that for  $\Lambda_\mp\text{CDM}$  cosmology with  $N_{\text{eff}} = 3.043$  we obtain very similar results, but with  $\chi^2_{\text{min}} = 4191.92$ .

are approximately at 0.72 and  $-0.74$ . It is easily seen that  $\Omega_{\Lambda_-}$  and  $z_c$  are highly correlated with each other, and show almost no correlation with the rest of the parameters. This means that changes in  $\Omega_{\Lambda_-}$  can be made compatible with observational data by a judicious choice of  $z_c$ : an earlier AdS to dS transition allows for larger (in magnitude)  $\Omega_{\Lambda_-}$  values. One can roughly quantify this relation by choosing a sample of the MCMC points with largest likelihood and modeling the relation between these parameters. For instance, choosing the top 1% points by likelihood, this relation is captured by

$$\Omega_{\Lambda_-} \approx -\frac{1}{2} z_c^2 + 1.33. \quad (3.2)$$

We end with two observations:

- From Table 1 it is straightforward to see that both  $\Lambda_s$ CDM and  $\Lambda_{\mp}$ CDM provide a solution of the  $M_B$  tension, for the two fiducial values of  $N_{\text{eff}}$ .
- Our results are consistent with and complement those recently reported in [72].

#### 4. Conclusions

$\Lambda_s$ CDM extends the  $\Lambda$ CDM concordance model of cosmology by promoting the assumption of a positive cosmological constant  $\Lambda$  to a rapidly sign-switching cosmological constant  $\Lambda_s$ , at critical redshift  $z_c$ . The innovative  $\Lambda_s$ CDM cosmology provides a profitable arena to simultaneously accommodate the  $H_0$  and  $S_8$  tensions. In this paper we explored the possibility of a similar transition, but between AdS and dS phases with different curvature radii. We have shown that  $z_c$  is strongly correlated with the vacuum energy  $\Omega_{\Lambda_-}$  in the AdS phase, and that there is no linear association between these variables and the other cosmological parameters. We have also shown that the cost of adding an additional parameter to the  $\Lambda_s$ CDM cosmological model does not improve the goodness of fit. Armed with our findings, we have demonstrated that for a proper choice of  $z_c$ , the vacuum energy in the dS phase may not necessarily be  $-\Omega_{\Lambda_-}$ , for comparable degree of conformity between the model prediction and experimental data.

#### CRediT authorship contribution statement

**Jorge F. Soriano:** Conceptualization, Investigation, Writing – review & editing. **Shimon Wohlberg:** Conceptualization, Investigation, Writing – review & editing. **Luis A. Anchordoqui:** Conceptualization, Investigation, Writing – review & editing.

#### Declaration of competing interest

The authors declare that they have no known competing financial interests or personal relationships that could have appeared to influence the work reported in this paper.

#### Acknowledgments

The work of L.A.A. is supported by the U.S. National Science Foundation (NSF), Grant PHY-2412679. S.W. is supported by the AstroCom NYC program through NSF Grant AST-2219090.

#### Data availability

Data will be made available on request.

#### References

- [1] K. Dutta, Ruchika, A. Roy, A.A. Sen, M.M. Sheikh-Jabbari, Beyond  $\Lambda$ CDM with low and high redshift data: implications for dark energy, *Gen. Relativity Gravitation* 52 (2) (2020) 15, [arXiv:1808.06623](#) [astro-ph.CO].
- [2] L. Visinelli, S. Vagnozzi, U. Danielsson, Revisiting a negative cosmological constant from low-redshift data, *Symmetry* 11 (8) (2019) 1035, [arXiv:1907.07953](#) [astro-ph.CO].
- [3] S. Di Gennaro, Y.C. Ong, Sign switching dark energy from a running barrow entropy, *Universe* 8 (10) (2022) 541, [arXiv:2205.09311](#) [gr-qc].
- [4] Y.C. Ong, An effective sign switching dark energy: Lotka–Volterra model of two interacting fluids, *Universe* 9 (10) (2023) 437, [arXiv:2212.04429](#) [gr-qc].
- [5] A. Gomez-Valent, J. Solà Peracaula, Phantom matter: A challenging solution to the cosmological tensions, *Astrophys. J.* 975 (1) (2024) 64, [arXiv:2404.18845](#) [astro-ph.CO].
- [6] A. Gómez-Valent, J. Solà Peracaula, Composite dark energy and the cosmological tensions, 2024, [arXiv:2412.15124](#) [astro-ph.CO].
- [7] S. Navas, et al., Particle Data Group Collaboration, Review of particle physics, *Phys. Rev. D* 110 (3) (2024) 030001.
- [8] N. Aghanim, et al., Planck Collaboration, Planck 2018 results. VI. Cosmological parameters, *Astron. Astrophys.* 641 (2020) A6, [arXiv:1807.06209](#) [astro-ph.CO], Erratum: *Astron. Astrophys.* 652 (2021) C4.
- [9] E. Abdalla, et al., Cosmology intertwined: A review of the particle physics, astrophysics, and cosmology associated with the cosmological tensions and anomalies, *JHEAp* 34 (2022) 49–211, [arXiv:2203.06142](#) [astro-ph.CO].
- [10] A.G. Riess, et al., A comprehensive measurement of the local value of the hubble constant with 1 km s<sup>-1</sup> Mpc<sup>-1</sup> uncertainty from the hubble space telescope and the SHOES Team, *Astrophys. J. Lett.* 934 (1) (2022) L7, [arXiv:2112.04510](#) [astro-ph.CO].
- [11] Y.S. Murakami, A.G. Riess, B.E. Stahl, W.D. Kenworthy, D.-M.A. Pluck, A. Macoreta, D. Brout, D.O. Jones, D.M. Scolnic, A.V. Filippenko, Leveraging SN ia spectroscopic similarity to improve the measurement of  $H_0$ , *JCAP* 11 (2023) 046, [arXiv:2306.00070](#) [astro-ph.CO].
- [12] C. Heymans, et al., KiDS-1000 Cosmology: Multi-probe weak gravitational lensing and spectroscopic galaxy clustering constraints, *Astron. Astrophys.* 646 (2021) A140, [arXiv:2007.15632](#) [astro-ph.CO].
- [13] D. Scolnic, et al., The Hubble Tension in our own backyard: DESI and the nearness of the coma cluster, *Astrophys. J. Lett.* 979 (1) (2025) L9, [arXiv:2409.14546](#) [astro-ph.CO].
- [14] E. Di Valentino, O. Mena, S. Pan, L. Visinelli, W. Yang, A. Melchiorri, D.F. Mota, A.G. Riess, J. Silk, In the realm of the Hubble tension—a review of solutions, *Cl. Quant. Grav.* 38 (15) (2021) 153001, [arXiv:2103.01183](#) [astro-ph.CO].
- [15] N. Schöneberg, G. Franco Abellán, A. Pérez Sánchez, S.J. Witte, V. Poulin, J. Lesgourgues, The  $H_0$  olympics: A fair ranking of proposed models, *Phys. Rep.* 984 (2022) 1–55, [arXiv:2107.10291](#) [astro-ph.CO].
- [16] L. Perivolaropoulos, F. Skara, Challenges for  $\Lambda$ CDM: An update, *New Astron. Rev.* 95 (2022) 101659, [arXiv:2105.05208](#) [astro-ph.CO].
- [17] S. Vagnozzi, Seven hints that early-time new physics alone is not sufficient to solve the hubble tension, *Universe* 9 (9) (2023) 393, [arXiv:2308.16628](#) [astro-ph.CO].
- [18] Ö. Akarsu, J.D. Barrow, L.A. Escamilla, J.A. Vazquez, Graduated dark energy: Observational hints of a spontaneous sign switch in the cosmological constant, *Phys. Rev. D* 101 (6) (2020) 063528, [arXiv:1912.08751](#) [astro-ph.CO].
- [19] Ö. Akarsu, S. Kumar, E. Özlüker, J.A. Vazquez, Relaxing cosmological tensions with a sign switching cosmological constant, *Phys. Rev. D* 104 (12) (2021) 123512, [arXiv:2108.09239](#) [astro-ph.CO].
- [20] O. Akarsu, S. Kumar, E. Özlüker, J.A. Vazquez, A. Yadav, Relaxing cosmological tensions with a sign switching cosmological constant: Improved results with Planck, BAO, and Pantheon data, *Phys. Rev. D* 108 (2) (2023) 023513, [arXiv:2211.05742](#) [astro-ph.CO].
- [21] O. Akarsu, E. Di Valentino, S. Kumar, R.C. Nunes, J.A. Vazquez, A. Yadav,  $\Lambda_s$ CDM model: A promising scenario for alleviation of cosmological tensions, 2023, [arXiv:2307.10899](#) [astro-ph.CO].
- [22] S.A. Adil, U. Mukhopadhyay, A.A. Sen, S. Vagnozzi, Dark energy in light of the early JWST observations: case for a negative cosmological constant? *JCAP* 10 (2023) 072, [arXiv:2307.12763](#) [astro-ph.CO].
- [23] N. Menci, S.A. Adil, U. Mukhopadhyay, A.A. Sen, S. Vagnozzi, Negative cosmological constant in the dark energy sector: tests from JWST photometric and spectroscopic observations of high-redshift galaxies, *JCAP* 07 (2024) 072, [arXiv:2401.12659](#) [astro-ph.CO].
- [24] A. Bernui, E. Di Valentino, W. Giarè, S. Kumar, R.C. Nunes, Exploring the  $H_0$  tension and the evidence for dark sector interactions from 2D BAO measurements, *Phys. Rev. D* 107 (10) (2023) 103531, [arXiv:2301.06097](#) [astro-ph.CO].
- [25] A. Gómez-Valent, A. Favale, M. Migliaccio, A.A. Sen, Late-time phenomenology required to solve the  $H_0$  tension in view of the cosmic ladders and the anisotropic and angular BAO datasets, *Phys. Rev. D* 109 (2) (2024) 023525, [arXiv:2309.07795](#) [astro-ph.CO].
- [26] J.D. Barrow, Sudden future singularities, *Cl. Quant. Grav.* 21 (2004) L79–L82, [arXiv:gr-qc/0403084](#).

- [27] E.A. Paraskevas, A. Cam, L. Perivolaropoulos, O. Akarsu, Transition dynamics in the  $\Lambda$ S $\Lambda$ CDM model: Implications for bound cosmic structures, *Phys. Rev. D* 109 (10) (2024) 103522, [arXiv:2402.05908](#) [astro-ph.CO].
- [28] S.W. Hawking, G.F.R. Ellis, *The Large Scale Structure of Space-Time*, in: Cambridge Monographs on Mathematical Physics, Cambridge University Press, 2023.
- [29] D. Lüst, E. Palti, C. Vafa, Ads and the Swampland, *Phys. Lett. B* 797 (2019) 134867, [arXiv:1906.05225](#) [hep-th].
- [30] L.A. Anchordoqui, I. Antoniadis, D. Lüst, Anti-de Sitter  $\rightarrow$  de Sitter transition driven by casimir forces and mitigating tensions in cosmological parameters, *Phys. Lett. B* 855 (2024) 138775, [arXiv:2312.12352](#) [hep-th].
- [31] O. Akarsu, A. De Felice, E. Di Valentino, S. Kumar, R.C. Nunes, E. Ozulker, J.A. Vazquez, A. Yadav,  $\Lambda$ <sub>s</sub>CDM cosmology from a type-II minimally modified gravity, 2024, [arXiv:2402.07716](#) [astro-ph.CO].
- [32] L.A. Anchordoqui, I. Antoniadis, D. Lüst, N.T. Noble, J.F. Soriano, From infinite to infinitesimal: Using the universe as a dataset to probe Casimir corrections to the vacuum energy from fields inhabiting the dark dimension, *Phys. Dark Univ.* 46 (2024) 101715, [arXiv:2404.17334](#) [astro-ph.CO].
- [33] Ö. Akarsu, A. De Felice, E. Di Valentino, S. Kumar, R.C. Nunes, E. Özülker, J.A. Vazquez, A. Yadav, Cosmological constraints on  $\Lambda$ S $\Lambda$ CDM scenario in a type II minimally modified gravity, *Phys. Rev. D* 110 (10) (2024) 103527, [arXiv:2406.07526](#) [astro-ph.CO].
- [34] A. Yadav, S. Kumar, C. Kibris, O. Akarsu,  $\Lambda$ <sub>s</sub>Cdm cosmology: Alleviating major cosmological tensions by predicting standard neutrino properties, 2024, [arXiv:2406.18496](#) [astro-ph.CO].
- [35] Y. Toda, W. Giarè, E. Özülker, E. Di Valentino, S. Vagnozzi, Combining pre- and post-recombination new physics to address cosmological tensions: Case study with varying electron mass and sign-switching cosmological constant, *Phys. Dark Univ.* 46 (2024) 101676, [arXiv:2407.01173](#) [astro-ph.CO].
- [36] S. Dwivedi, M. Högsås, 2D BAO vs 3D BAO: solving the hubble tension with an alternative cosmological model, 2024, [arXiv:2407.04322](#) [astro-ph.CO].
- [37] L.A. Anchordoqui, I. Antoniadis, D. Bielli, A. Chatrabhuti, H. Isono, Thin-wall vacuum decay in the presence of a compact dimension meets the  $H_0$  and  $S_8$  tensions, 2024, [arXiv:2410.18649](#) [hep-th].
- [38] O. Akarsu, B. Bulduk, A. De Felice, N. Katurci, N.M. Uzun, Unexplored regions in teleparallel  $f(T)$  gravity: Sign-changing dark energy density, 2024, [arXiv:2410.23068](#) [gr-qc].
- [39] M.S. Souza, A.M. Barcelos, R.C. Nunes, Ö. Akarsu, S. Kumar, Mapping the  $\Lambda$ <sub>s</sub>CDM scenario to  $f(t)$  modified gravity: Effects on structure growth rate, *Universe* 11 (1) (2025) 2, [arXiv:2501.18031](#) [astro-ph.CO].
- [40] S. Weinberg, *Cosmology*, Oxford University Press, 2008.
- [41] E. Hubble, A relation between distance and radial velocity among extra-galactic nebulae, *Proc. Nat. Acad. Sci.* 15 (1929) 168–173.
- [42] M. Kamionkowski, A. Kosowsky, The Cosmic microwave background and particle physics, *Ann. Rev. Nucl. Part. Sci.* 49 (1999) 77–123, [arXiv:astro-ph/9904108](#).
- [43] W. Hu, S. Dodelson, Cosmic microwave background anisotropies, *Ann. Rev. Astron. Astrophys.* 40 (2002) 171–216, [arXiv:astro-ph/0110414](#).
- [44] A. Kosowsky, M. Milosavljevic, R. Jimenez, Efficient cosmological parameter estimation from microwave background anisotropies, *Phys. Rev. D* 66 (2002) 063007, [arXiv:astro-ph/0206014](#).
- [45] G. Steigman, D.N. Schramm, J.E. Gunn, Cosmological limits to the number of massive leptons, *Phys. Lett. B* 66 (1977) 202–204.
- [46] M. Cielo, M. Escudero, G. Mangano, O. Pisanti, Neff in the standard model at NLO is 3.043, *Phys. Rev. D* 108 (12) (2023) L121301, [arXiv:2306.05460](#) [hep-ph].
- [47] L.A. Anchordoqui, H. Goldberg, Neutrino cosmology after WMAP 7-year data and LHC first  $Z'$  bounds, *Phys. Rev. Lett.* 108 (2012) 081805, [arXiv:1111.7264](#) [hep-ph].
- [48] G. Mangano, G. Miele, S. Pastor, T. Pinto, O. Pisanti, P.D. Serpico, Relic neutrino decoupling including flavor oscillations, *Nuclear Phys. B* 729 (2005) 221–234, [arXiv:hep-ph/0506164](#).
- [49] P.F. de Salas, S. Pastor, Relic neutrino decoupling with flavour oscillations revisited, *JCAP* 07 (2016) 051, [arXiv:1606.06986](#) [hep-ph].
- [50] J.J. Bennett, G. Buldgen, M. Drewes, Y.Y.Y. Wong, Towards a precision calculation of the effective number of neutrinos  $N_{\text{eff}}$  in the Standard Model I: the QED equation of state, *JCAP* 03 (2020) 003, [arXiv:1911.04504](#) [hep-ph], Addendum: *JCAP* 03 (2021) A01.
- [51] K. Akita, M. Yamaguchi, A precision calculation of relic neutrino decoupling, *JCAP* 08 (2020) 012, [arXiv:2005.07047](#) [hep-ph].
- [52] J. Froustey, C. Pitrou, M.C. Volpe, Neutrino decoupling including flavour oscillations and primordial nucleosynthesis, *JCAP* 12 (2020) 015, [arXiv:2008.01074](#) [hep-ph].
- [53] J.J. Bennett, G. Buldgen, P.F. De Salas, M. Drewes, S. Gariazzo, S. Pastor, Y.Y.Y. Wong, Towards a precision calculation of  $N_{\text{eff}}$  in the Standard Model II: Neutrino decoupling in the presence of flavour oscillations and finite-temperature QED, *JCAP* 04 (2021) 073, [arXiv:2012.02726](#) [hep-ph].
- [54] D. Camarena, V. Marra, On the use of the local prior on the absolute magnitude of type Ia supernovae in cosmological inference, *Mon. Not. R. Astron. Soc.* 504 (4) (2021) 5164–5171, [arXiv:2101.08641](#) [astro-ph.CO].
- [55] G. Efstathiou, To  $H_0$  or not to  $H_0$ ? *Mon. Not. R. Astron. Soc.* 505 (3) (2021) 3866–3872, [arXiv:2103.08723](#) [astro-ph.CO].
- [56] D. Camarena, V. Marra, A new method to build the (inverse) distance ladder, *Mon. Not. R. Astron. Soc.* 495 (3) (2020) 2630–2644, [arXiv:1910.14125](#) [astro-ph.CO].
- [57] D. Blas, J. Lesgourgues, T. Tram, The cosmic linear anisotropy solving system (CLASS) II: Approximation schemes, *JCAP* 07 (2011) 034, [arXiv:1104.2933](#) [astro-ph.CO].
- [58] J. Lesgourgues, The cosmic linear anisotropy solving system (CLASS) I: Overview, 2011, [arXiv:1104.2932](#) [astro-ph.IM].
- [59] T. Brinckmann, J. Lesgourgues, MontePython 3: boosted MCMC sampler and other features, *Phys. Dark Univ.* 24 (2019) 100260, [arXiv:1804.07261](#) [astro-ph.CO].
- [60] C.P. Robert, The Metropolis-Hastings algorithm, 2015, [arXiv:1504.01896](#) [stat.CO].
- [61] A. Gelman, D.B. Rubin, Inference from iterative simulation using multiple sequences, *Statist. Sci.* 7 (1992) 457–472.
- [62] N. Aghanim, et al., Planck Collaboration, Planck 2018 results. V. CMB power spectra and likelihoods, *Astron. Astrophys.* 641 (2020) A5, [arXiv:1907.12875](#) [astro-ph.CO].
- [63] R.C. Nunes, S.K. Yadav, J.F. Jesus, A. Bernui, Cosmological parameter analyses using transversal BAO data, *Mon. Not. R. Astron. Soc.* 497 (2) (2020) 2133–2141, [arXiv:2002.09293](#) [astro-ph.CO].
- [64] D. Brout, et al., The Pantheon+ Analysis: Cosmological constraints, *Astrophys. J.* 938 (2) (2022) 110, [arXiv:2202.04077](#) [astro-ph.CO].
- [65] K. Kuijken, et al., The fourth data release of the kilo-degree survey: ugri imaging and nine-band optical-IR photometry over 1000 square degrees, *Astron. Astrophys.* 625 (2019) A2, [arXiv:1902.11265](#) [astro-ph.GA].
- [66] B. Giblin, et al., KiDS-1000 catalogue: Weak gravitational lensing shear measurements, *Astron. Astrophys.* 645 (2021) A105, [arXiv:2007.01845](#) [astro-ph.CO].
- [67] H. Hildebrandt, et al., KiDS-1000 catalogue: Redshift distributions and their calibration, *Astron. Astrophys.* 647 (2021) A124, [arXiv:2007.15635](#) [astro-ph.CO].
- [68] M. Asgari, et al., KiDS Collaboration, KiDS-1000 Cosmology: Cosmic shear constraints and comparison between two point statistics, *Astron. Astrophys.* 645 (2021) A104, [arXiv:2007.15633](#) [astro-ph.CO].
- [69] R.E. Smith, J.A. Peacock, A. Jenkins, S.D.M. White, C.S. Frenk, F.R. Pearce, P.A. Thomas, G. Efstathiou, H.M.P. Couchmann, VIRGO Consortium Collaboration, Stable clustering, the halo model and nonlinear cosmological power spectra, *Mon. Not. R. Astron. Soc.* 341 (2003) 1311, [arXiv:astro-ph/0207664](#).
- [70] S. Bird, M. Viel, M.G. Haehmelt, Massive neutrinos and the non-linear matter power spectrum, *Mon. Not. R. Astron. Soc.* 420 (2012) 2551–2561, [arXiv:1109.4416](#) [astro-ph.CO].
- [71] A. Mead, J. Peacock, C. Heymans, S. Joudaki, A. Heavens, An accurate halo model for fitting non-linear cosmological power spectra and baryonic feedback models, *Mon. Not. R. Astron. Soc.* 454 (2) (2015) 1958–1975, [arXiv:1505.07833](#) [astro-ph.CO].
- [72] Ö. Akarsu, L. Perivolaropoulos, A. Tsikoundoura, A.E. Yükselci, A. Zhuk, Dynamical dark energy with AdS-to-dS and dS-to-dS transitions: Implications for the  $H_0$  tension, 2025, [arXiv:2502.14667](#) [astro-ph.CO].